The GMT Dynamic Optical Simulation

R. Conan[†], A. Bouchez[†], F. Quiros–Pacheco[†], and B. McLeod[‡]

[†]Giant Magellan Telescope Organisation, 155 South Lake Avenue, Pasadena, CA, USA
[‡]Harvard Smithsonian Astrophysical Observatory, 60 Garden St, Cambridge, MA, USA

ABSTRACT

The Giant Magellan Telescope (GMT) is a gregorian 25.5-meter diameter primary mirror (M1) made of 7 8.4-meter diameter circular aspheric segments. The secondary mirror (M2) is a 1/8th down-scale model of M1 made of 7 1- meter diameter segments. Each segments has positionners to adjust its 6 rigid body motions. The figure of M1 segment is controlled with 44 bending modes and M2 segments are deformed using 672 actuators. In the active and adaptive operation modes of the GMT, around a dozen wavefront sensors (WFS) are selectively used to monitor the optical aberrations building-up into the telescope. A dedicated control system feeds back the WFS measurements to the mirrors actuators to deliver image quality optimized for the field of view of each scientific instrument. This paper describes the GMT Dynamic Optical Simulation (DOS) tool. DOS integrates the optical and mechanical model of the telescope together with the control system. DOS is a cloud-based optical propagation software package with build-in models for both geometric and Fourier optics and a full control algorithm development environment.

Keywords: ray tracing, wavefront control, active optics, adaptive optics

1. INTRODUCTION

The Giant Magellan Telescope[3] (GMT) will be a Gregorian 25.5-meter diameter telescope with a primary mirror (M1) made of 7 8.4-meter diameter circular aspheric segments. The secondary mirror (M2) is made of 7 1-meter diameter segments. Each segments has positionners to adjust its 6 rigid body motions. The figure of M1 segments is controlled with 44 bending modes and the adaptive M2 segments can be deformed using 672 actuators. In the active and adaptive operation modes of the GMT, around a dozen wavefront sensors (WFS) are selectively used to monitor the optical aberrations of the telescope. A dedicated control system feeds back the WFS measurements to the mirrors actuators to deliver image quality optimized for the field of view of each scientific instrument

The Dynamic Optical Simulation (DOS) is a simulation environment that brings together optics, mechanical motions, surface deformations and control models applied to the GMT active and adaptive[2] optics systems. At its core is CEO (Cuda–Engined Optics), a CUDA package performing the most time consuming computing tasks by running multi–threaded code on GPUs. CEO functionalities are available through a python interface that consits in cython wrapper classes around C++ structures.

CEO is emulating the GMT M1 and M2 segments, the sensors and the propagation of the light. CEO is

- moving and reshaping each segment independently,
- tracing rays through the atmosphere,
- tracing rays through M1 and M2 to the telescope exit pupil,
- computing the wavefront from the ray tracing propagation,
- Fourier propagating the wavefront through the wavefront sensors.

Further author information: (Send correspondence to R. Conan)
R. Conan: E-mail: rconan@gmto.org, Telephone: 1 626 204 0507

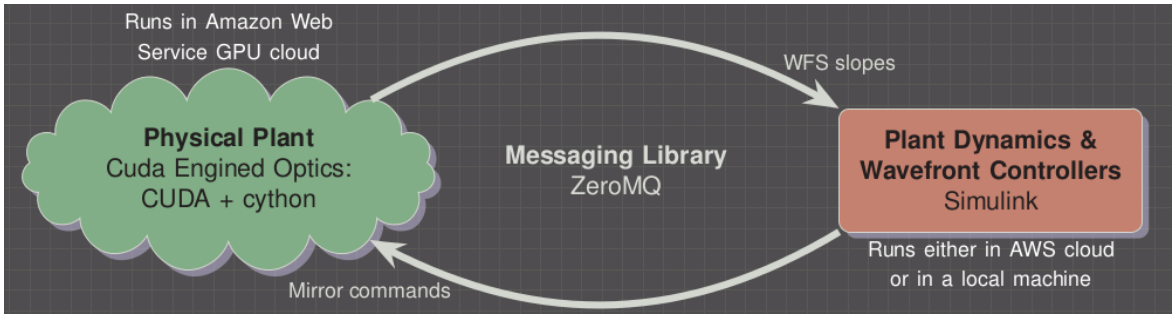

Figure 1. DOS workflow

CEO is a standalone tool within the DOS that can be used either in batch mode or interactively. The interactive interface of choice is Jupyter, a web browser–based notebook. Jupyter allows to write code in a browser locally while running the code remotely on a GPU–enabled machine.

While simple control models are written with python, the most elaborated control models are developed with Simulink. The WFS outputs are passed from CEO to Simulink and the derived and filtered mirror commands in Simulink are send back to CEO. The messaging library ZeroMQ is used to make the link between CEO and Simulink (Fig. 1).

In the following sections, a simple feedback controller between the active optics WFSs and GMT M1 and M2 segments is described. Section 2 describes the light propagation process as modeled in CEO. The model of the GMT M1 and M2 mirrors is detailed in Sec. 3. The procedure to build the control system with Simulink and Jupyter is given ins Sec. 4.

2. OPTICAL PROPAGATION MODEL

The steps required for a complete optical propagation from the source to the detector are:

1. rays are traced from the source through M1 and M2 to the telescope exit pupil,
2. the ray optical path differences in the exit pupil are converted into a wavefront,
3. the wavefront is propagated to the detector plane using a Fourier optics propagation model,
4. the detector frame is computed
5. photon noise and read–out noise are added to the frame
6. the frame is processed to get the WFS measurements.

2.1 Ray tracing

In CEO, each optical surface is defined with the following equation

$$F(x,y,z,a_i,N) = z - z_0 - C(\rho) - \sum_{i=1}^{N} a_i Z_i(\rho,\theta) = 0. \tag{1}$$

and

$$C(\rho,c,\kappa) = \frac{c\rho^2}{1+\sqrt{1-\kappa c^2\rho^2}}. \tag{2}$$

with $\rho^2 = (x-x_0)^2 + (y-y_0)^2$, where (x_0, y_0, z_0) is the coordinate of the origin of the surface. $C(\rho, c, \kappa)$ is the expression for the conic surface where c and κ are the vertex curvature and the conic parameter, respectively. $Z_i(\rho,\theta)$ is a Zernike polynomial of order i with coefficient a_i. The coordinates (x, y, z) are given by the intersection

of a ray with the optical surface[7] . The Zernike polynomials are computed on the fly, using a fast recursive method[1] .

Each segment of M1 and M2 have a different optical surface, all given by Eq. (1). All the segments of a mirror, M1 or M2, have the same (c, κ) values but different (x_0, y_0, z_0) and a_i parameters. For each segment the coordinates (x, y, z) is defined in a different coordinate system (See Sec. 3).

The rays originate from a plane above M2, coming from the direction of the guide star they refer to. The first ray tracing is done from the plane of origin to M2, which acts here as a stop i.e. only the rays outside of M2 footprint will be valid for the subsequent ray tracings.

The next ray tracing is done from the plane of origin to M1. The intersections of the rays with the M1 segments are computed. The optical path lengths from the previous surface are derived. The chief ray is propagated for a perfectly aligned and shaped M1. The optical path differences of the rays, defined as the difference between the optical path differences of a ray and the chief ray, are also saved. Next, the rays are traced from M1 to M2 following the same procedure that for M1.

The last ray tracing is from M2 to the exit pupil(Fig. 3). The exit pupil location is computed as the intersection of the chief ray with the optical axis where the optical axis is the imaginary line emanating from the vertex of M1 central segment and normal to the surface. The surface the rays intersect with at the exit pupil is a sphere whose origin is the intersection of the chief ray and the focal plane, and that is tangent to the exit pupil[5] . The origin of the sphere is also the location of the image of the source in the focal plane.

2.2 Fourier optics propagation

The optical path difference computed at the exit pupil is written into the phase of the source wavefront. The amplitude of the wavefront is filtered according to the vignetting of the rays during the ray tracing process.

As we are considering only the case of imaging sources at infinity from the wavefront sensor perspective, the wavefront propagation is performed with the Fraunhofer approximation meaning that the image in the focal plane is simply the Fourier transform of the complex amplitude in the pupil plane[4] .

A zero–padded discrete Fourier transform is applied to the wavefront meaning that if the wavefront resolution is $n \times n$, the Fourier transform is $\alpha n \times \alpha n$ with the zero–padding factor $\alpha \geq 2 \in \mathcal{Z}$. The image size can be set to any size N. If $\alpha n > N$, the Fourier transform is cropped to the specified size N, if $\alpha n < N$, the Fourier transform is padded with zeros up to N. The square modulus of the Fourier transform of size $N \times N$ can be binned down by a factor $\beta \geq 1 \in \mathcal{Z}$ to form the detector frame of size $N/\beta \times N/\beta$. At the detector, the pixel scale is given by:

$$\frac{\beta\lambda}{\alpha d}$$

and the field-of-view is

$$N\frac{\lambda}{\alpha d}$$

with λ the wavelength of the source, and d is the lenslet pitch.

Photon noise and read–out noise are added to the detector frame before processing the frame to get the measurements.

3. GMT OPTICAL MODEL

Both mirrors, M1 and M2, are represented with the same model but with a different set of parameters (Table 1). Critical to the model is the definition of different coordinate systems (CS) for the mechanical and optical surfaces. The main CS is the global CS (GCS) centered at the vertex of the central M1 segment which is also the vertex of the parent optics surface.

Fig. 2 shows the genitor–offspring relationship between the different CSs. The 7 segments are placed inside the GCS as shown in Fig. 4. For each segment a new CS, the rigid body CS, is defined centered at the origin of the segment. Each rigid body CS is tilted inward, the z–axis pointed towards the z–axis of the GCS at a slight

	Full	Clear	r_i	β	L	c	κ	Height
M1	8.417	8.365	0.292	13.602	8.710	1/36	0.0017143	0
M2	1.0477	1.0415	0	-14.777	1.08774	-1.0/4.1639	0.2830722	20.2625

Table 1. M1 and M2 parameters: full and clear aperture, the ratio between the central segment hole diameter and its clear aperture diameter, the inclination angle of the rigid body CSs, the distance to the center of the outer segment, the vertex radius, the conic parameter and the height of the mirror.

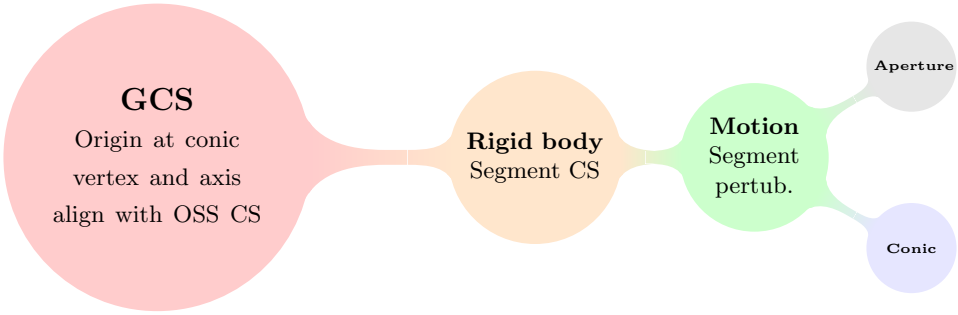

Figure 2. Coordinate system spawning diagram.

angle. The origins $[x_O, y_O, z_O]$ of the rigid body CS are given with respect to the global coordinate system which origin is at the vertex of the parent conic surface:

$$x_{O,k} = L\cos(\theta_{O,k}), \quad (3)$$
$$y_{O,k} = L\sin(\theta_{O,k}), \quad (4)$$
$$z_O = h + C(L, c, \kappa), \quad (5)$$

with $\theta_{O,k} = \pi(3-2k)/6, \forall k \in [0, 5]$, $x_{O,6} = y_{O,6} = 0$, h the height of the mirror and $C(L, c, \kappa)$ is given by Eq. (2). In addition to the change of origin with respect to the GCS, the rigid body CSs are rotated around the z–axis of $-k\pi/3$ radians and then tilted around the x–axis of β. The orientation of the rigid body CS is given by the 3 Euler angles $(\gamma_x = \beta, \gamma = 0, \gamma_z = -k\pi/3)$.

The 6 degree of motions of each segment are set by the motion CS that is defined with respect to the rigid body CS. For unperturbed segments, both the rigid body CS and the motion CS coincide.

Then, inside the motion CS, the CS of the optical surface of each segment (Eq. (1)), the conic CS, is defined. Both the motion CS and the conic CS share the same origin and for unperturbed segments, the x, y and z axes of the conic CS are parallel to the x, y and z axes of the GCS. The Euler angles of the conic CSs are $(\gamma_x = \beta, \gamma = 0, \gamma_z = -k\pi/3)$. The origins $(x_{0,k}, y_{0,k}, z_{0,k})$ of the optical surfaces are different for each segment and are given by

$$x_{0,k} = -L\cos(\theta_{O,k}), \quad (6)$$
$$y_{0,k} = -L\sin(\theta_{O,k}), \quad (7)$$
$$z_{0,k} = -C(L, c, \kappa), \quad (8)$$

The segment aperture has also is own CS defined with respect to the motion CS. The apertures are directly above the segments at $z = C(R, c, \kappa)$ such as they rest on the rim of the segments, with R the radius of the clear aperture.

The ray tracing flowchart for M1 and M2 mirrors is given in Fig. 3. Each ray enters and exits the procedure in the GCS. The coordinates of a ray are transformed 3 times: first, into the rigid body CS of the selected segment, second, in the motion CS to account for the segment motion and then into the aperture CS. If the ray does not hit the segment aperture, it moves to the next segment or exits the routine. If the ray is not vignetted by the aperture, the coordinates of a ray are transformed from the motion CS into the conic CS. The ray tracing consists in the intersection of the ray with the segment and the reflection from the segment. It can be performed only in the conic CS.

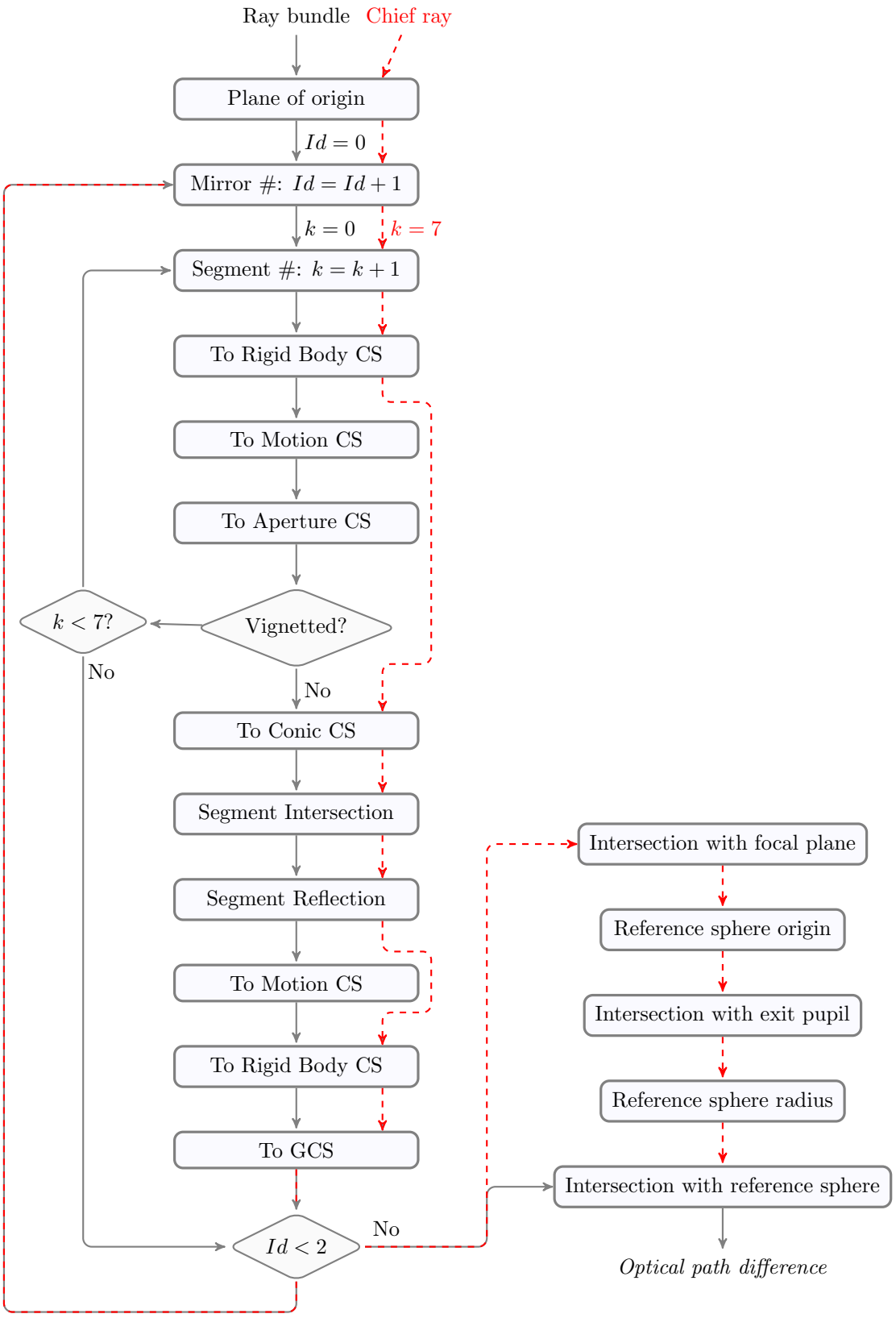

Figure 3. Ray tracing flowchart for GMT M1 and M2 mirrors.

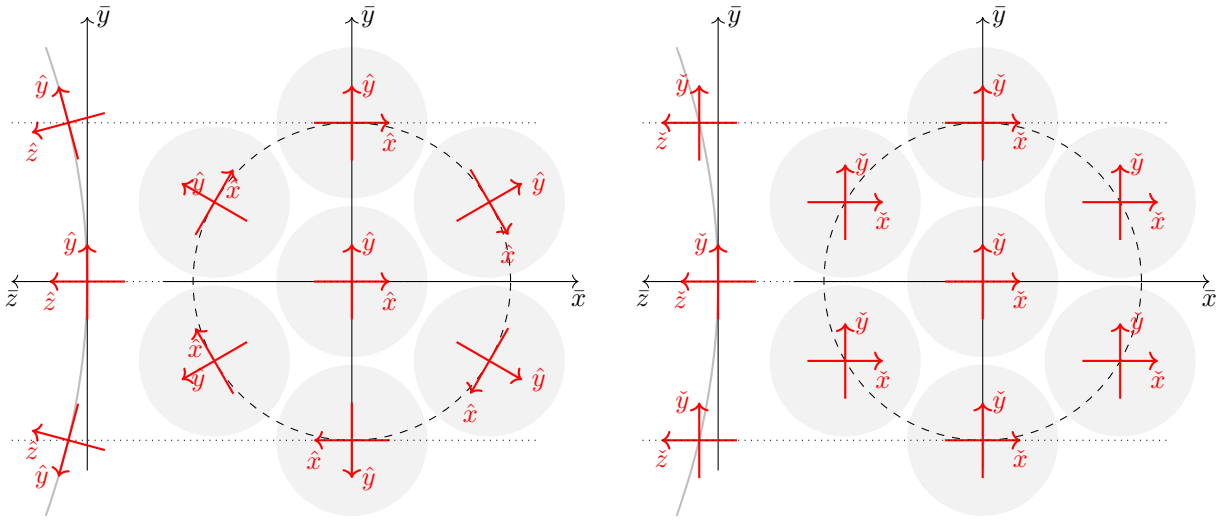

Figure 4. Sidecut and top view of the mirror model with the GCS $(\bar{x}, \bar{y}, \bar{z})$ and the 7 rigid body motion CSs $(\hat{x}, \hat{y}, \hat{z})$ on the right and the 7 conic CSs $(\check{x}, \check{y}, \check{z})$ on the left.

The chief ray is also propagated but only through the, ideally aligned, central segment of the mirrors. The location of the exit pupil, situated directly after M2, is derived from the intersection of the chief ray with the optical axis. The intersection of the chief ray with the focal plane gives the position of the object in the image plane. A reference sphere centered on the object in the image plane and tangent to the exit pupil is introduced. The optical path length of all the rays (including the chief ray) to the reference sphere is computed. The optical path differences of the rays are derived from the differences between the optical paths of the rays and the optical path of the chief ray.

4. CONTROL

A simple model of the active optics of the GMT is presented in the following. It consists of:

- the GMT model as described in Sec. 3,
- 3 off–axis WFSs in R band at 9.5' off–axis,
- 1 on–axis imager in R band.

There is no atmosphere and detector noise in the model. All the perturbations are static.

The control model block diagram is given in Fig. 5. Only the tip and tilt of M2 segments are controlled with a type I integrator (Fig. 6) with a gain $g = 0.5$. M1 and M2 segment position and orientation are set in the *M1 prms* and *M2 prms* blocks and are send to CEO on the GPU server with the *zmq_pub* blocks. After reception of the segment commands, CEO updates each segment location and propagates the light to the WFS. The WFS slopes are send back to Simulink and are received with the *zmq_sub* block. In Simulink, the slopes are converted into M2 segment tip–tilt with the reconstruction matrix *M2tt*. *M2tt* is the pseudo–inverse of the tip–tilt interaction matrix between M2 and the WFSs. The calibration procedures are run in CEO. The derived command are filtered by the integrator, formatted to the proper vector size and subtracted from the initial perturbations

4.1 M2 tip–tilt perturbation

Uniformly randomly distributed tip and tilt between +1 and -1 arcsec were applied to each M2 segments. Fig. 7 shows the corresponding input wavefront aberration in the top–left and corrected wavefront in the top–right. The time evolution of the wavefront error rms is shown in the bottom graph. Note that the corrected wavefront is the wavefront expected for a perfectly aligned telescope with a WFE RMS of 0.79nm.

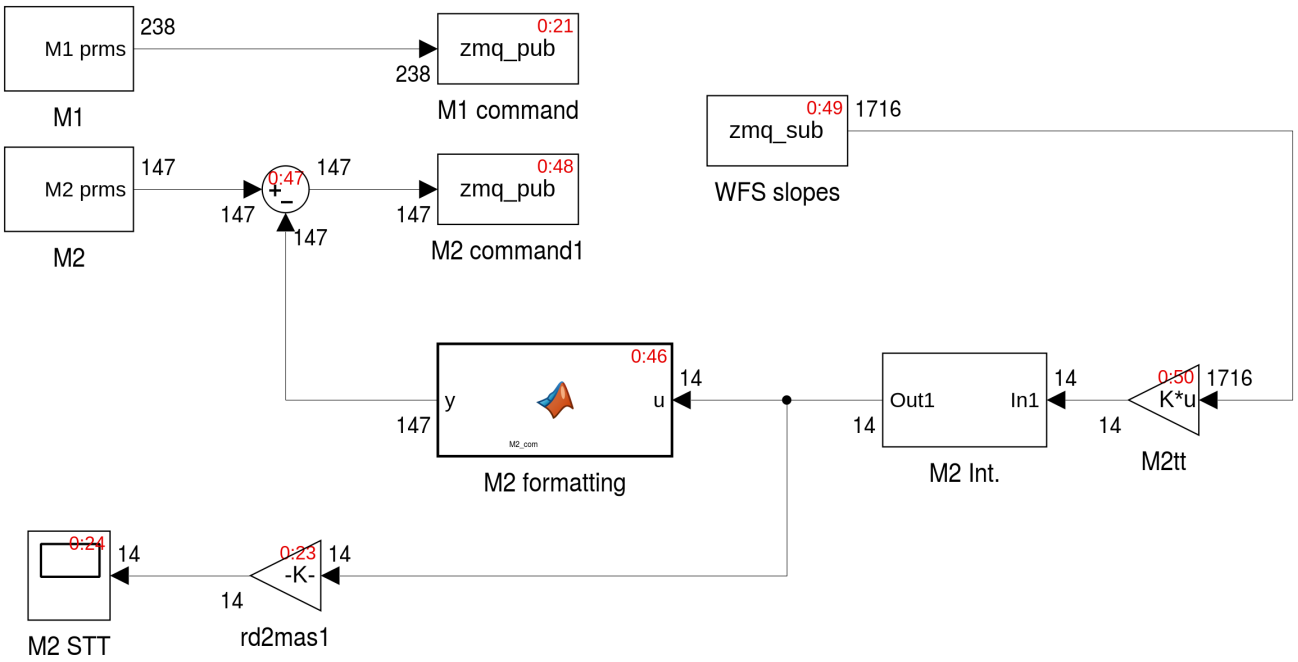

Figure 5. Simulink control block diagram.

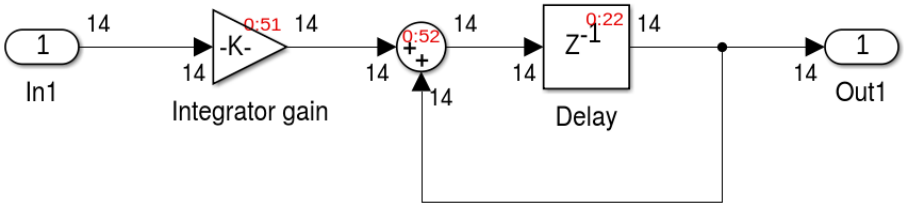

Figure 6. Integrator block diagram (M2 Int.) in the Simulink block diagram (Fig. 5).

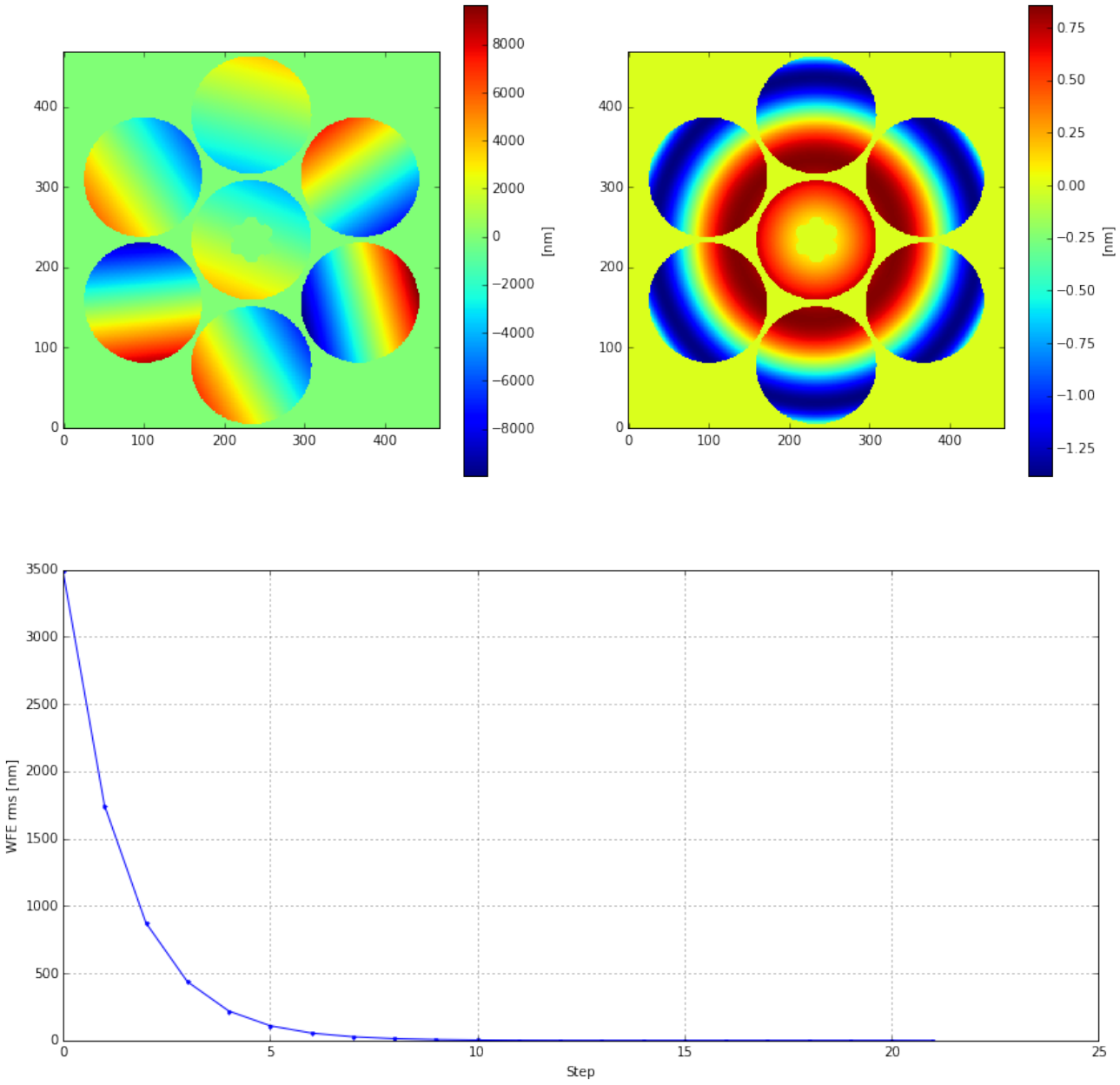

Figure 7. M2 segment tip–tilt correction in closed loop (see text for details).

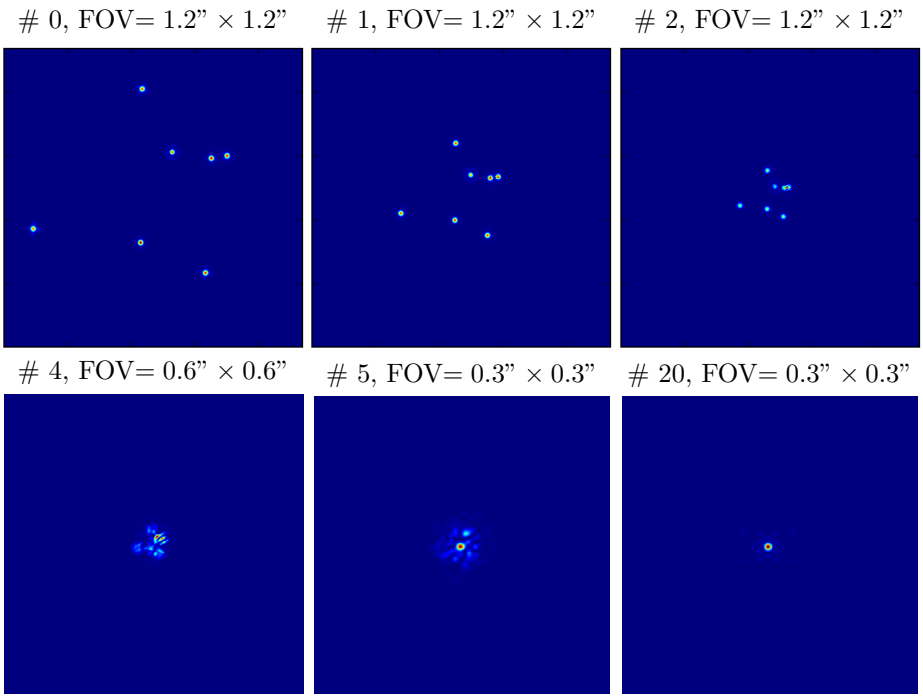

Figure 8. Time evolution of the on–axis PSF for the M2 tip–tilt only model (Sec. 4.1).

The on–axis images at different iteration in the loop are displayed in Fig. 8 showing how progressively the image is transformed from 7 8m–diameter PSFS to a single 25m–diameter PSF.

4.2 M1 global tip–tilt perturbation

In this example, only a global tip–tilt is applied to M1, M1 and M2 mirrors are both phased, and there are no perturbations applied to any M2 segments. The M1 tip and tilt amplitude are 30mas and -50mas, respectively. The results from the closed–loop run using the control model of Fig. 5 and Fig. 6 are shown in Fig. 9. The top left and top right images are, respectively, the resulting PSF and the corresponding wavefront aberration across the GMT pupil. The middle graph shows the time evolution of the wavefront error RMS. The bottom image shows the residual slopes in mas of the 3 WFSs.

The loop rapidly converges to a residual WFE of 3.1 micron that is mainly piston across the segments. This is expected as the aberration for the peripheral segments of M1 are a combination of piston and tilts and M2 only corrects for the tilts. The slopes of the WFS exhibit tip and tilt patterns meaning that a residual focus between each M1/M2 segment pair is also present. This is simply because a piston of a given segment induced a change in the focal plane distance of that segment pair. So for a fixed focal plane, one is left with some focus aberrations.

The shape of the PSF can be explained with a simple model of the GMT pupil:

$$P(\vec{r}) = \Pi\left(\frac{r}{D_s}\right) + \Pi\left(\frac{r}{D_s}\right) * \sum_{k=0}^{5} \delta(\vec{r} - \vec{r}_k)\exp(ip_k), \tag{9}$$

with $\vec{r}_k = L\exp(2i\pi k/6 + \pi/2)$, p_k the piston of segment k, $D_s = 8$m and

$$\begin{aligned} \Pi(r) &= 1, \text{ if } r < 1/2, \\ &= 0, \text{ elsewhere.} \end{aligned}$$

The corresponding PSF is

$$I(\vec{f}) = A(\vec{f})Q(\vec{f}), \tag{10}$$

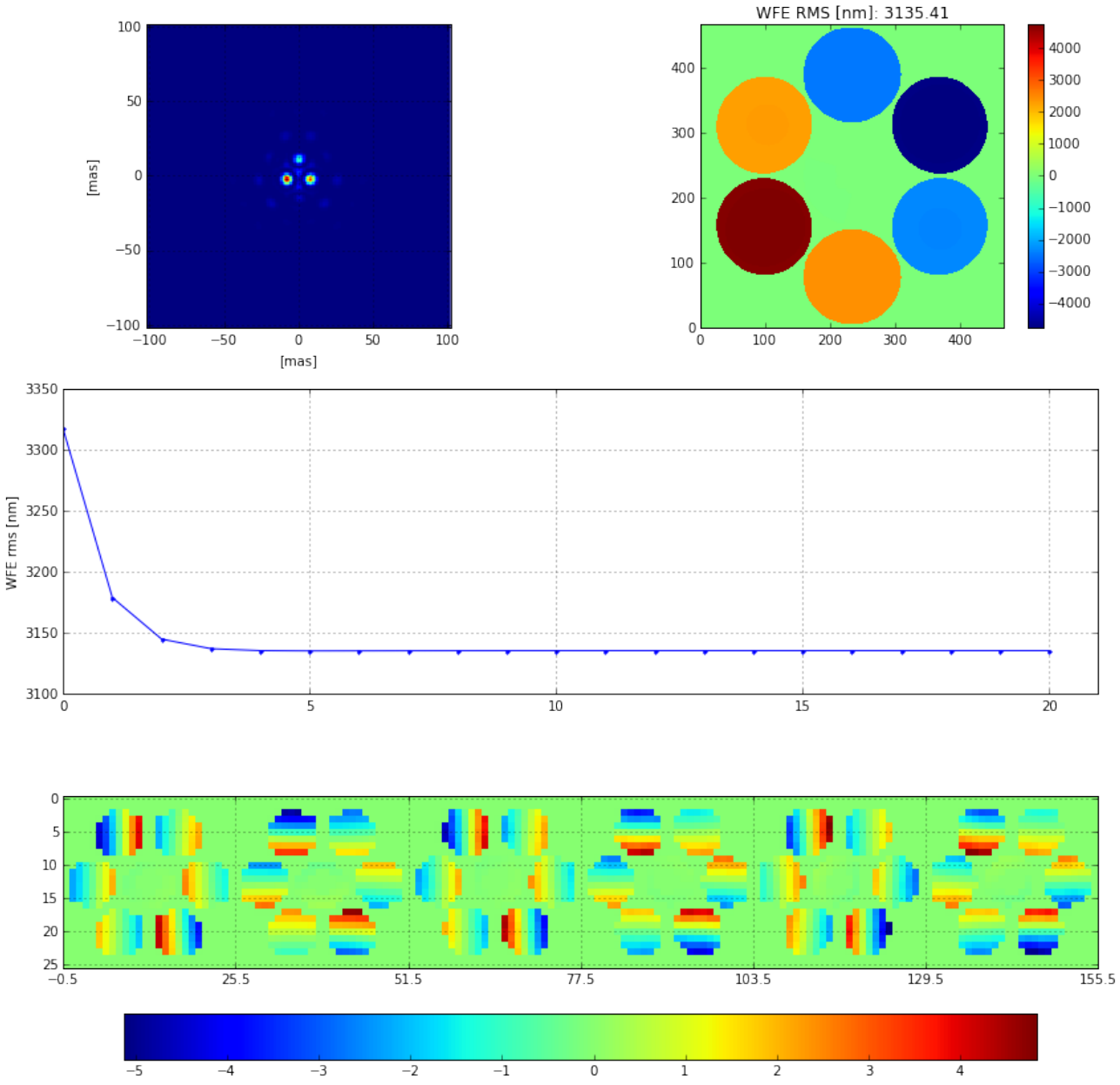

Figure 9. M1 global tip–tilt correction in closed loop (see text for details).

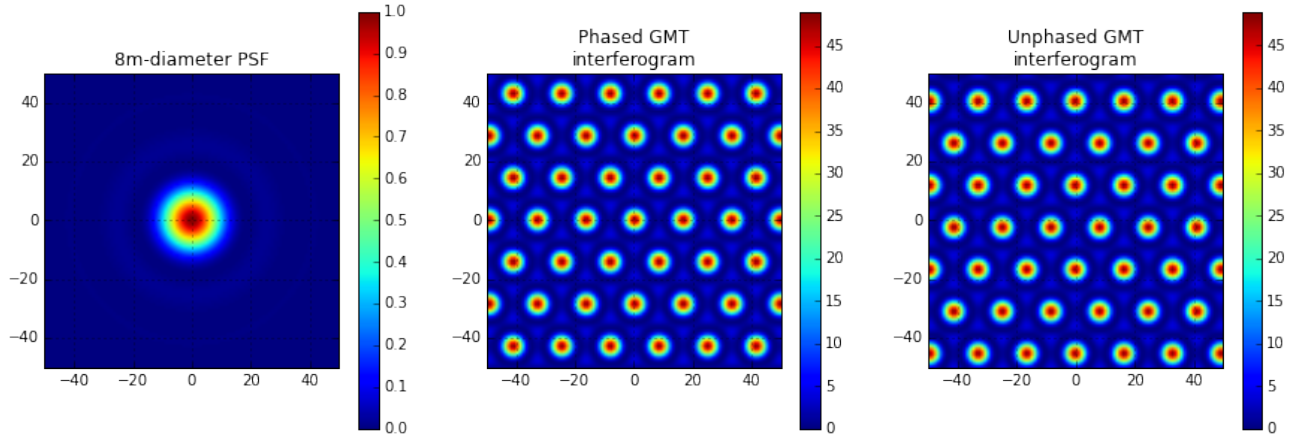

Figure 10. $A(\vec{f})$ on the left, phased $Q(\vec{f})$ in the middle and unphased $Q(\vec{f})$ on the right.

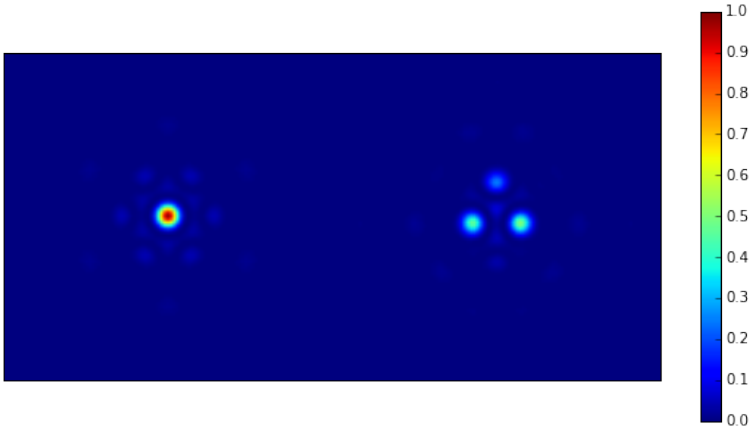

Figure 11. Phased (right) and unphased (left) PSFs.

where

$$A(\vec{f}) = \left| \frac{2J_1(\pi D_s f)}{\pi D_s f} \right|^2 \quad \text{and} \quad Q(\vec{f}) = \left| 1 + \sum_{k=0}^{5} \exp(2i\pi \vec{f} \cdot \vec{r}_k) \exp(ip_k) \right|^2 .$$

$A(\vec{f})$ is the Airy function i.e. the PSF of a 8–m diameter circular aperture and $Q(\vec{f})$ is the GMT interferogram. Fig. 10 shows the function $A(\vec{f})$ on the right and the function $Q(\vec{f})$, $\forall p_k = 0$ in the middle and with the residual piston from Fig. 9 on the left. The corresponding phased and unphased PSF are given in Fig. 11. The principle of image formation in the GMT is better understood if one considers the GMT as a giant Fizeau interferometer. With only piston error in the segments of M1 and M2, the PSF of the GMT is the product of an 8m–diameter PSF modulated by the 7–segment–induced interferogram. The misalignment of the interferogram with respect to the segment PSF is the reason for the speckled image, each speckle having the FWHM of a 25–m diameter aperture. For the unphased PSF, despite a Strehl of 4.6%, the maximum intensity is still half the peak intensity of the phased PSF. The resolution is also preserved but every unresolved star in the field will appear as the same triplet.

5. CONCLUSION

The Dynamic Optical Simulation (DOS) environment brings together optics, mechanics and control applied to the GMT active and adaptive optics systems. The hardware emulation and light propagator components have been written for GPU machines within a software package called CUDA–Engined Optics (CEO). The GMT control algorithms are developed with Simulink. The commands and measurements are passed back and forth between the controller in Simulink and the hardware emulator in CEO closely mimicking the control architecture envisioned for the GMT.

Active optics and phasing[6] control systems are in development and already part of the DOS. The control systems of the AO modes will also be integrated into the DOS. A dedicated effort is underway to port the dynamic component of the solid models of M1 and M2 into the DOS using the Simulink interface.

REFERENCES

[1] Chee-Way Chong, P. Raveendran, and R. Mukundan. A comparative analysis of algorithms for fast computation of zernike moments. *Pattern Recognition*, 36:731–742, 2003.

[2] A. Bouchez et al. Preliminary Design of the Giant Magellan Telescope Adaptive Optics System. In *Adaptive Optics for Extremely Large Telescopes III*, May 2013.

[3] P. McCarthy et al. Scientific Promise and Status of the Giant Magellan Telescope Project. In *Adaptive Optics for Extremely Large Telescopes III*, May 2013.

[4] J.W Goodman. *Introduction to Fourier Optics*. McGraw–Hill, Boston, 1988.

[5] D. Malacara and Z. Malacara. *Handbook of Optical Design Second Edition*. Marcell Dekker, New York, 2004.

[6] F. Quiros-Pacheco, R. Conan, B. McLeod, B. Irarrazaval, and A. Bouchez. Wavefront control simulations for the Giant Magellan Telescope: Field-dependent segment piston control. In *Adaptive Optics for Extremely Large Telescopes IV*, July 2015.

[7] G. H. Spencer and M. V. R.K. Murty. General ray tracing procedure. *J. Opt. Soc. Am.*, 52(6):672–678, 1962.